

Fracture resistance estimation of elastic ceramics in edge flaking: EF baseline

G.A. Gogotsi^{*}, V.I. Galenko, S.P. Mudrik, B.I. Ozersky, V.V. Khvorostyany, T.A. Khristevich

Pisarenko Institute for Problems of Strength, 2, Timiryazevskaya Str., 01014 Kiev, Ukraine

Received 27 July 2009; received in revised form 12 November 2009; accepted 1 December 2009

Available online 6 January 2010

Abstract

The fracture resistance of single-phase oxide and nonoxide ceramics was studied in flaking the specimen edge with a Rockwell indenter (EF test method) and in bar flexure (SEVNB method). The fracture resistance F_R and fracture toughness K_{Ic} are shown to be proportional, the plot with the F_R – K_{Ic} coordinates is termed the EF base diagram, in which the EF baseline is constructed. It was revealed that the fracture resistance of ceramics was not influenced by chip scar shapes on the specimen edge. The data points for inelastic ceramics with a lower EF barrier to the onset of fracture lay below the EF baseline in the base diagram, while the data points for glasses and ceramics with a higher barrier were located above it.

The EF test method is appropriate for comparative evaluation of fracture resistance of ceramics and verification of estimates obtained by other methods.

© 2009 Elsevier Ltd. All rights reserved.

Keywords: Fracture; Mechanical properties; Al_2O_3 ; Si_3N_4 ; Edge chipping

1. Introduction

The fracture behaviour of brittle materials is usually evaluated by conventional methods based on flexure of rectangular bars with a stress concentrator and/or impression of a Vickers indenter into the polished specimen surface. For these methods, the critical stress intensity factor K_{Ic} (fracture toughness¹) serves as the fracture criterion. However, quite reliable information on the ability of brittle materials to resist fracture cannot always be obtained, e.g.,^{2,3} which exerts negative influence on correct fracture resistance estimates. Therefore, a method based on flaking the specimen edge with a Rockwell indenter⁴ deserves further examination. This method is somewhat similar to that used by our remote ancestors in choosing stones for arms and tools.⁵ It is not based on any concepts of the ideally brittle material of linear fracture mechanics¹ or on the model of a crack shape originated in the specimen on indentation.⁶ These models are often greatly simplified as compared to the true material properties.

One of the versions of this method⁷ known as the edge fracture (EF) test method^{8,9,a} provides fracture resistance estimates

for conventional elastic ceramics that are proportional to those obtained by the SEVNB method. This relation is known as the *baseline*.⁹ However, the EF fracture behaviour of such ceramics has not been studied extensively enough, though these materials are widely used for different purposes. This situation can cast doubt on the reliability of such a fundamental relation as the baseline, while its practical application opens the way for gaining new information on the behaviour of different brittle materials in fracture. To confirm the above, additional investigations were performed. Their results are outlined in the present communication.

2. Materials and methods

2.1. Ceramics

Linear elastic single-phase isotropic ceramics almost consistent with the concept of the ideally brittle material of linear fracture mechanics¹ were chosen for the investigation. Sintered scandia and yttria (S and Y) from the Eastern Institute of Refractories (Russia),¹¹ Duralbit-90 alumina A-1 (1987) and A-2 (2005) from Industrie Bitossi S.p.A. (Italy), summarized in Table 1, were used for testing. The structure of these ceramics is shown in micrographs (Fig. 1). Hot-pressed silicon nitride HP Si_3N_4 ⁹ specimens and silicon nitride SN speci-

^{*} Corresponding author. Tel.: +380 44 285 44 64; fax: +380 44 286 16 84.

E-mail address: ggogotsi@ipp.kiev.ua (G.A. Gogotsi).

^a It was compared with other versions in Ref. 10.

Table 1
Characteristics of examined materials.

Ceramics	Density (g/cm ³)	Elastic modulus E (GPa)	Strength (MPa)	Fracture toughness K_{Ic} (MPa m ^{1/2})	Fracture resistance F_R (N/mm)	
					All results	$L = 100\text{--}400\text{ }\mu\text{m}$
S	3.79	218	110	1.49 ± 0.04	150 ± 34 (134)	145 ± 31 (118)
Y	4.90	193	75	3.14 ± 0.06	336 ± 65 (105)	329 ± 63 (95)
A-1	3.49	232	269	2.93 ± 0.08	267 ± 42 (113)	272 ± 37 (95)
A-2	3.57	266	329	3.01 ± 0.09	300 ± 56 (140)	290 ± 49 (122)
SN	3.13	269	396	4.10 ± 0.06	409 ± 68 (96)	407 ± 64 (87)
HPSN	3.30	—	—	4.16 ± 0.16	417 ± 36 (81)	418 ± 37 (79)
A-999	3.86	398	473	3.90 ± 0.16	362 ± 72 (93)	353 ± 57 (73)

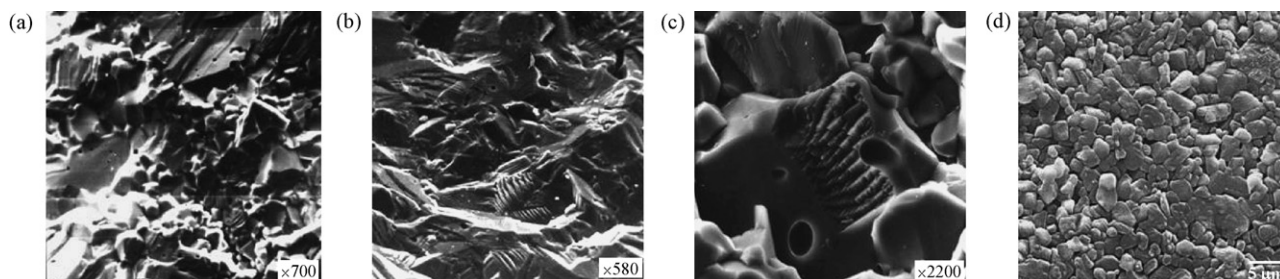


Fig. 1. Micrographs of fractured surfaces on S (a), Y (b), A-1 (c), and polished surface of A-2 (d) specimens.

mens, cut out from the cover of the diesel engine cylinder from Toyomenka Kaisha, Ltd. (Japan), were also employed in the experiments. Alumina ceramics A-999,^{12,13} having the structure similar to that shown in Fig. 1d, were used as a reference material.^b

As is known, all the above materials are prone to catastrophic fracture after the onset of crack propagation. Since their mechanical behaviour was studied earlier, any unexpected phenomena during experiments were not observed.

2.2. Procedures

The fracture toughness of ceramics was evaluated by the single-edge V-notch beam (SEVNB) method in three-point flexure (20-mm span) of specimens with a 3 mm × 4 mm cross-section¹² (differs from the standard procedure¹³ only in a smaller span size). For this purpose a CeramTest device (Gobor Ltd., Ukraine) mounted on a universal test machine was used. Its cross-head speed was 0.5 mm/min. The device is equipped with a rigid dynamometer located under the test specimen. It features two steel membranes that ensure precision displacement of the loading rod, as well as a facility on the lower loading support for perpendicular arrangement of the specimen axis relative to the axes of loading rollers.¹⁵

A V-notch was prepared with a special machine. In the specimens, a 200- μm prenotch was cut out with a diamond saw, then a V-notch was polished out with a razor blade distributing a 1–2- μm diamond paste. Its radius did not usually exceed 5–10 μm . The radius and depth were measured on an Olympus

51MX binocular microscope using a Quick PHOTO MICRO 2.3 program.

Specimen fragments formed in those tests were used for further experiments to maintain comparability of results.

Edge flaking tests were performed by the edge fracture (EF) method also with a CeramTest device. But instead of the loading support, the X–Y table with the system of specimen clamping was installed, in its loading rod, indenters were fixed (earlier this technique was employed in studying the fracture behaviour of zirconia crystals¹⁶). Test specimens were glued to photographic glasses clamped on the X–Y table. The indentation point near the specimen edge was chosen with a magnifying glass, after that it was flaked. The flaking was effected with a Rockwell C-Scale standard conical diamond indenter (Gilmore Diamond Tools, Inc., USA). This operation was multiple-repeated for all the specimens (Fig. 2a). The fracture distance L from the extreme point on the chip scar to its edge was measured by an Olympus 51MX microscope (Fig. 2b). These experimental values served for evaluating the fracture resistance of ceramics.

Such a procedure of measuring the fracture distance is a specific feature of the EF test method, making it different from other similar techniques,^{10,17} in which the loading point is chosen with a microscope, thus, the fracture distance is measured from the contact point of the indenter with the specimen to its edge. Fracture loads P_f , which were registered by PC, and corresponding fracture distances L were used to construct P_f – L relations (fracture diagrams). The P_f/L ratio was termed the fracture resistance F_R .

Since this investigation was aimed at gaining exhaustive information on the fracture behaviour of ceramics, the EF procedure became the basic test method. For these experiments indenters were made to special order, providing precise round-

^b This material was tested in Round Robin,¹⁴ thus, it can be used by its participants to check the reliability of our results.

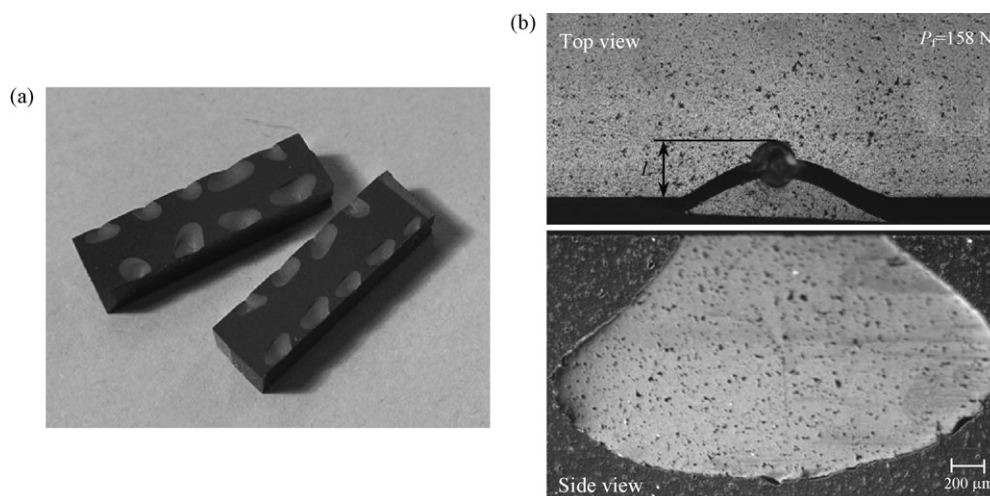


Fig. 2. Tested SN specimens (a) and fracture zone on an SN specimen with a chip, not separated from its edge (b).

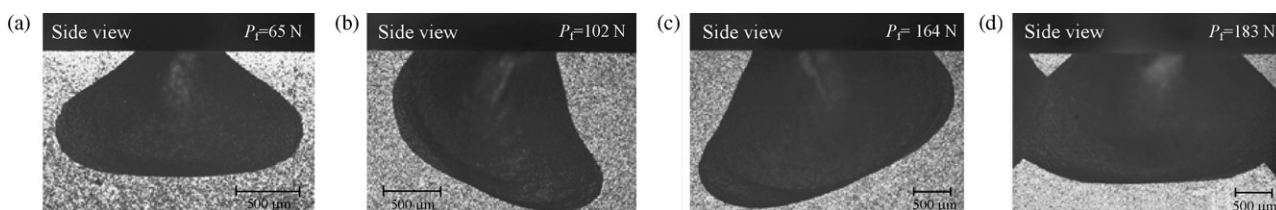


Fig. 3. Chip scars on the side surface of A-999 specimens: symmetrical (a), asymmetric (b and c), and overlapping (d).

ing of its tip (200 μm). This characteristic was not practically controlled during our first experiments.⁹

Sharp edges of specimens with a lower fracture resistance were formed by their “package grinding” that turned out to be rather effective for glass specimen preparing.¹⁸ In this case one specimen side is first polished, then specimens are glued along these sides into a package, after that its top surfaces are ground and polished. Thus, a high sharpness of the edge was obtained and possible chipping defects on the specimen edges were excluded.

3. Results and discussion

The results obtained in this study have contributed to better understanding of the local fracture behaviour of examined ceramics.

Strength and elastic moduli data (test method is described in Ref. 19) as well as fracture toughness values together with EF test results of examined ceramics are summarized in Table 1. Micrographs of the fracture surfaces of ceramics became the source of additional information (Fig. 1).

First test results for fractured specimens revealed that chip scars on their side surfaces acquired different shapes. They were symmetrical and of other shapes (Figs. 2a and 3a–c), even partially overlapping each other (Fig. 3d), and several chips were not separated from specimen edges (Fig. 2b). Such fracture behaviour is most often observed at small fracture distances L (for S, Y, and SN ceramics, their number was 38, 27, and 9, respectively, for the rest of ceramics that phenomenon was not

observed). However, fracture diagrams (Fig. 4) demonstrated that all experimental data irrespective of chip scar shapes were located along the straight line, i.e., fracture resistance estimates are not influenced by chip scar shapes. In examined cases the fracture resistance of ceramics was probably controlled by their ability to withstand the onset of avalanche-like crack propagation. The direction of their propagation can vary because of small inaccuracies in perpendicularity of indenter movement relative to the specimen surface, occasional defects on their surfaces, local structural nonuniformities, etc.

The experimental data were plotted in the F_R – K_{Ic} diagram (EF base diagram^{9,c}) and approximated by the straight EF baseline (Fig. 5). As is seen in this figure, the data points for examined ceramics were located close enough to the above line.^{8,9} The comparison of this line with that presented in Ref. 9 shows that they are little different, though the latter was constructed by experimental results without account of the indenter tip radius and specimen edge sharpness. Thus, F_R for S ceramics was 143 ± 27 N/mm and became 150 ± 34 N/mm, for Y ceramics it was 316 ± 76 N/mm and became 336 ± 55 N/mm, repeated tests of Si_3N_4 demonstrated satisfactory repeatability of experimental results (395 ± 30 N/mm and 416 ± 77 N/mm^d). The above confirms that the EF method can be employed in a conventional mechanical laboratory where it is quite difficult to maintain a high technical level of test requirements.

^c Earlier the designation EF was not used.

^d Data points for these ceramics see in Fig. 5.

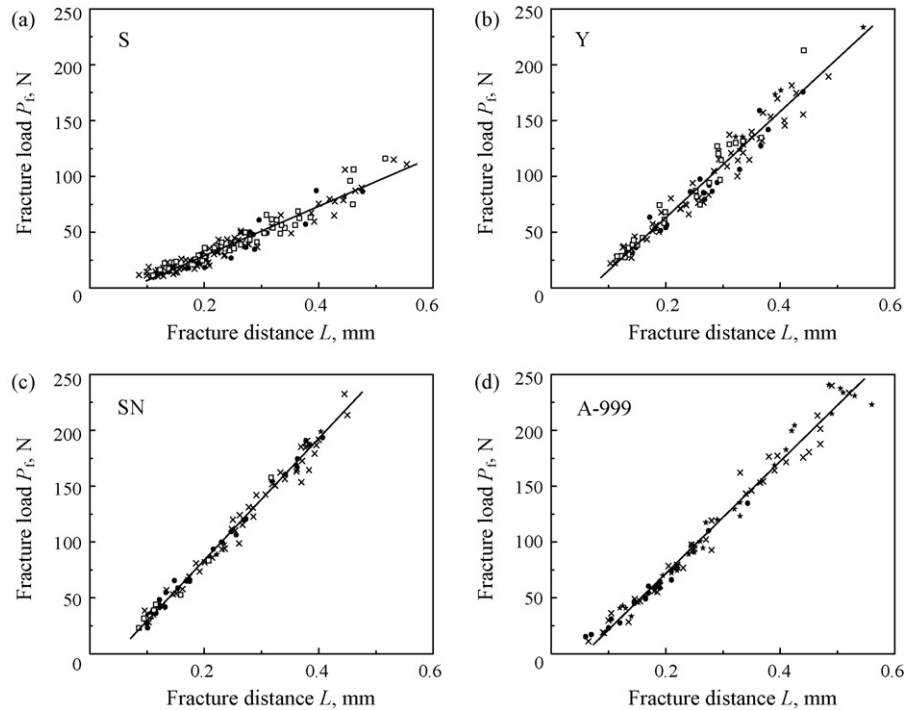


Fig. 4. Fracture diagrams for S, Y, SN, and A-999 ceramics: data points for symmetrical (●), asymmetric (×), overlapping (★), and not separated (□) chip scars.

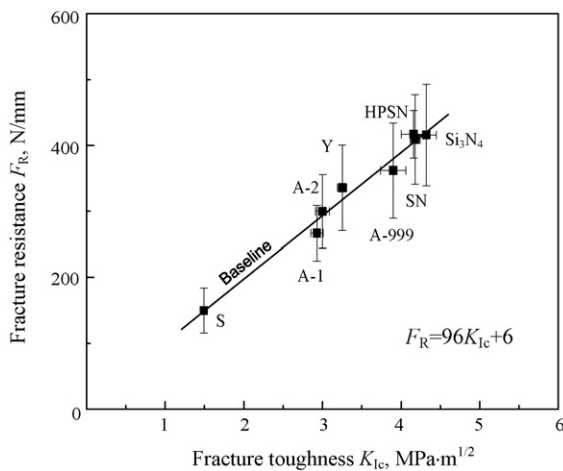


Fig. 5. EF baseline for all experimental results.

It might be well to compare the EF baseline with other similar relationships, which were analyzed, e.g., in Ref. 20–23. For instance, the relationship (Fig. 6a) between the edge toughness (ratio of load fracturing the specimen edge with a Rockwell indenter to the distance from the specimen edge to its contact point with the specimen surface) and critical strain energy release rate G_{Ic} for different brittle materials (from glasses to hard metals), shown in Ref. 20,21, is entirely inappropriate for glasses and ceramics (Fig. 6b).²⁴ Data for sapphire²⁰ are also consistent with the same critical strain energy release rate values (Fig. 6), though it is an anisotropic material, and these values should be different in different crystallographic directions. Similar relationships were obtained in the tests with a sharp Vickers indenter,^{22,23} they correspond to the F_{RV} – K_{Ic} relation, located in the EF base diagram at a smaller slope.¹⁰ Thus, the above publications are not associated with our approach to edge flaking using a blunt Rockwell indenter and the EF baseline construction.

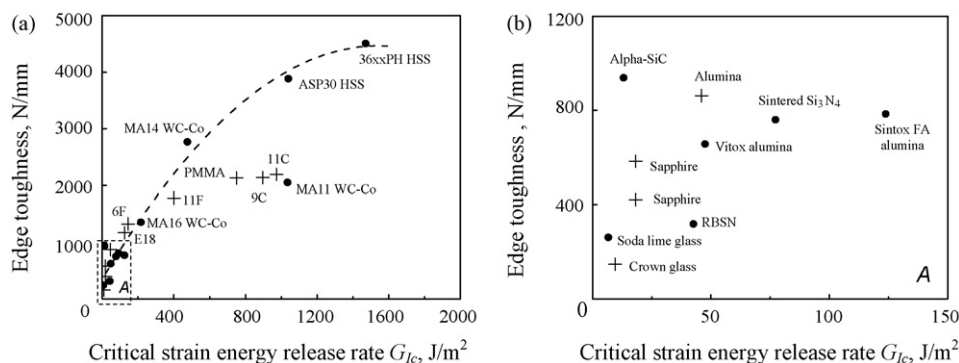
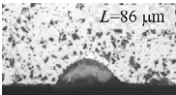
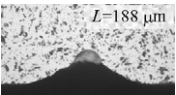
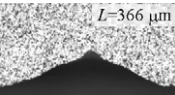
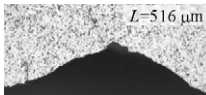


Fig. 6. Edge toughness vs. critical strain energy release rate: a - all results, b - A zone results.^{20,21}

Table 2
Chip scar shapes in the indentation direction.

Ceramics	Fracture resistance F_R (N/mm)			
				
	Group 1	Group 2		Group 3
S	127 ± 30 (16) ^a	133 ± 22 (14)	149 ± 32 (75)	175 ± 33 (29)
Y	251 ± 43 (8)	282 ± 60 (18)	344 ± 52 (56)	387 ± 42 (23)
A-1	226 ± 45 (19)	235 ± 39 (13)	282 ± 32 (69)	286 ± 27 (12)
A-2	238 ± 29 (29)	266 ± 31 (32)	330 ± 41 (64)	363 ± 19 (15)
HPSN	408 ± 52 (9)	414 ± 43 (14)	420 ± 28 (49)	415 ± 50 (9)
SN	327 ± 42 (21)	356 ± 49 (13)	440 ± 39 (46)	467 ± 43 (16)
A-999	268 ± 57 (13)	283 ± 44 (8)	372 ± 49 (50)	435 ± 30 (22)

^a Number of chip scars.

Analysis of the fracture diagrams (Fig. 4) shows that with longer fracture distances the scatter of experimental data becomes somewhat wider, and nonlinearity of the initial range of the fracture diagram must not be ruled out (Fig. 4a). For explaining this phenomenon, an effort was made to examine chip scars developed in the indentation direction (Table 2). They can easily be divided into the three groups. The first group is the chip scars in the form of a circle fraction, formed by the primary ring crack²⁵ under the indenter ($L < 100 \mu\text{m}$). The chip scars of the second group are the primary crack and two secondary cracks that extend it and come out to the specimen edge. The chip scars of the third group ($L > 350\text{--}450 \mu\text{m}$) feature the appearance of the horizontal portion in the initial section of the secondary cracks.^{2,18} Taking into consideration the above, the fracture diagram was cut off and its range corresponding to the fracture distance $L = 100\text{--}400 \mu\text{m}$ was taken as optimum for further analysis. In this case the baseline (Fig. 7) changes inconsiderably.²⁶

Further analysis should take account of the fact that the critical stress intensity factor K_{Ic} , proposed by Irwin²⁷ and recognized as the fracture criterion, can be comparable with the

Griffith surface energy γ_{ef} ²⁸ for the ideally brittle material using his critical strain energy release rate concept $G_{Ic} = K_{Ic}^2/E = 2\gamma_{ef}$ (E is the elastic modulus).¹ In our case, the fracture resistance F_R was proportional to the critical stress intensity factor K_{Ic} . Thus, proportionality between F_R and K_{Ic} values for ceramics that are similar to the ideally brittle material confirms that these criteria do not contradict each other. Therefore, the $F_R\text{--}K_{Ic}$ relation (EF baseline) may be used for evaluating the validity of K_{Ic} estimates in different tests. For this purpose, additional EF experiments should be performed and their results together with K_{Ic} data plotted in the EF baseline. Fracture toughness measurements are valid only in the case when the data points of both experiments practically coincide with this line.

It should be noted that the less the mechanical behaviour of ceramics is consistent with that of the ideally brittle material, the farther their data points from the baseline (Fig. 7), e.g., inelastic phase-transformed partially stabilized Mg-PSZ (MS) ceramics,²⁵ a silicon nitride particulate ceramic composite,²⁹ or a microlaminated composite Ti_3SiC_2 .¹⁰ So, their fracture diagrams can be nonlinear, stress–strain curves for these materials are often nonlinear ($\chi < 1$),³⁰ thus, their fracture resistance should not be estimated using the linear fracture mechanics concepts.¹ In the strict sense, their fracture criterion should be J-integral rather than the critical stress intensity factor K_{Ic} .^{31,25} Data points that do not coincide with the baseline, lying above it (Fig. 7), are typical of materials displaying the effect of a high barrier to the onset of fracture^{9,10} (higher resistance to the nucleation of an initial crack), which is inherent in boron and silicon carbide ceramics,⁷ as well as technical and optical glasses¹⁸ (Fig. 7). Analysis of test results²¹ using the EF approach⁹ (Fig. 8) leads also to a similar conclusion. For this purpose, data points for conventional linear elastic RBSN, Vitox alumina, and sintered Si_3N_4 ceramics should be connected by the straight line, similar to our baseline. Then data points for soda lime glass and Alpha-SiC should be plotted in the “base diagram”, it turns out that they fall much above this line, which is indicative of the existence of a fracture barrier.

To make the EF baseline generally accepted (standard), ceramics totally corresponding to the ideally brittle material of linear fracture mechanics should additionally be tested.

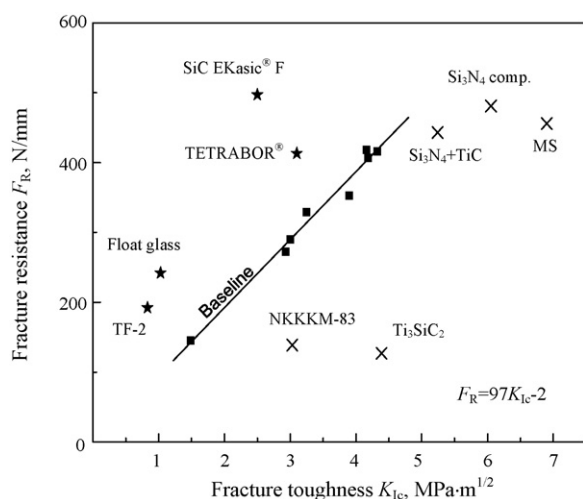


Fig. 7. EF base diagram with data points for ceramics exhibiting fracture barriers of different levels ($L = 100\text{--}400 \mu\text{m}$).

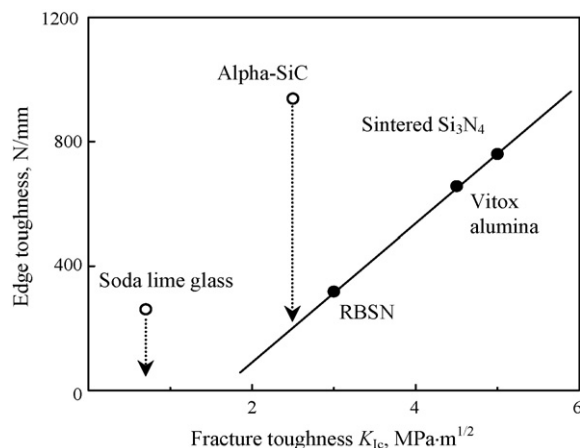


Fig. 8. Fracture barrier estimation for several materials.²¹

4. Conclusion

The existence of the proportional relation between the fracture resistance F_R and fracture toughness K_{Ic} for linear elastic homogeneous ceramics (similar to the ideally brittle material of linear fracture mechanics) has been confirmed. This relationship has been termed the EF baseline.

It has been shown that the economically attractive and easy-to-apply EF test method can be employed instead of recognized methods for fracture resistance estimation of conventional ceramics. It does not require special test equipment and large-size specimens.

The EF baseline is useful for establishing the reliability of fracture toughness estimates of ceramics tested by accepted methods, it may also be appropriate for approximate division of materials by their resistance to the onset of fracture.

References

- Anderson T. *Fracture mechanics: fundamentals and applications*. 3th ed. Boca Raton: CRC Press; 1995.
- Gogotsi GA, Galenko VI, Mudrik SP, Ozersky BI, Khvorostyany VV, Khristevich TA. Fracture behaviour of Y-TZP ceramics: new outcomes. *Ceram Int* 2010;**36**:345–50.
- Quinn GD, Bradt RC. On the Vickers indentation fracture toughness test. *J Am Ceram Soc* 2007;**90**:673–80.
- Almond E, McCormick N. Constant geometry edge-flaking of brittle materials. *Nature* 1986;**321**:53–5.
- Brumm A, Aziz F, Bergh G, Morwood M, Moore M, Kurniawan I, et al. Early stone technology on Flores and its implications for *Homo floresiensis*. *Nature* 2006;**444**:624–8.
- Fischer-Cripps AC. *Introduction to contact mechanics*. 2nd ed. New York: Springer; 2007.
- Gogotsi G, Mudrik S, Rendtel A. Sensitivity of silicon carbide and other ceramics to edge fracture: method and results. In: Lara-Curzio E, Readey M, editors. *28th International Conference on Advanced Ceramics and Composites: A, Ceramic Engineering & Science Proceedings*, 25. American Ceramic Society; 2004. p. 237–46.
- Gogotsi G. Fracture resistance of ceramics: direct measurements. *Adv Sci Technol* 2006;**45**:95–100.
- Gogotsi GA. Fracture resistance of ceramics: base diagram and R-line. *Strength Mater* 2006;**38**:261–70.
- Gogotsi GA, Mudrik SP. Fracture barrier estimation by the edge fracture test method. *Ceram Int* 2009;**35**:1871–5.
- Gogotsi GA. Thermal stress behavior of yttria, scandia and AlN ceramics. *Ceram Int* 1990;**5**:31–5.
- Gogotsi GA. Fracture toughness of ceramics and ceramic composites. *Ceram Int* 2003;**29**:777–84.
- ISO 23146. Fine ceramics (advanced ceramics, advanced technical ceramics). Test Methods for Fracture Toughness of Monolithic Ceramics. Single-edge V-notch Beam (SEVNB) Method. ISO, Switzerland, 2008.
- Kübler J. Fracture toughness of ceramics using the SEVNB method. Round Robin VAMAS Report No. 37/ESIS Document D2-99. EMPA, Dübendorf, Switzerland, Swiss Federal Laboratories for Materials Testing and Research, September 1999.
- Radin NN, Gogotsi GA, and Kuzema YuA. Device for Testing Specimens in Flexure. Author's Certificate of the USSR No. 1419294, May 22, 1985.
- Gogotsi GA, Dub SN, Lomonova EE, Ozersky BI. Vickers and Knoop indentation behavior of cubic and partially stabilized zirconia crystals. *J Eur Ceram Soc* 1995;**15**:405–13.
- Gogotsi G, Mudrik S, Galenko V. Evaluation of fracture resistance of ceramics: edge fracture tests. *Ceram Int* 2007;**33**:315–20.
- Gogotsi GA, Mudrik SP. Fracture behaviour of glasses: EF approach. *J. Non-Crystal. Sol.*, submitted for publication.
- Gogotsi GA. Deformation behavior of ceramics. *J Eur Ceram Soc* 1991;**7**:87–92.
- McCormick N, Almond E. Edge flaking of brittle materials. *J Hard Mater* 1990;**1**:25–51.
- Morrell R, Gant AJ. Edge chipping of hard materials. *Int J Refr Metal Hard Mater* 2001;**19**:293–301.
- Chai H, Lawn B. A universal relation for edge chipping from sharp contacts in brittle materials: a simple means of toughness evaluation. *Acta Mater* 2007;**55**:2555–61.
- Petit F, Vandeneede V, Cambier F. Ceramic toughness assessment through edge chipping measurements—influence of interfacial friction. *J Eur Ceram Soc* 2009;**29**:2135–41.
- Gogotsi GA, Galenko VI, Ozersky BI, Khristevich TA, Karban VI. Direct determination of fracture resistance of ceramics by the edge fracture method. *Zavod Lab* 2007;**3**:49–53.
- Gogotsi GA. Fracture behaviour of Mg-PSZ ceramics: comparative estimations. *Ceram Int* 2009;**35**:2735–40.
- Gogotsi GA. Flaking toughness of advanced ceramics: ancient principle revived in modern times. *Mater Res Innov* 2006;**10–2**(45–47):179–86.
- Irwin GR. Analysis of stresses and strains near the end of a crack traversing a plate. *Appl Mech* 1955;**24**:361–4.
- Griffith A. The phenomena of rupture and flow in solids. *Philos Trans R Soc* 1920;**221A**:163–98.
- Gogotsi GA. Mechanical behaviour of a silicon nitride particulate ceramic composite. *Ceram Int* 2009;**35**:1109–14.
- Gogotsi GA. The use of brittleness measure (χ) to represent mechanical behavior of ceramics. *Ceram Int* 1989;**15**:127–9.
- Evans AG, Faber KT. Crack-growth resistance of microcracking brittle materials. *J Am Ceram Soc* 1984;**67**:255–60.